

Reorganization and Caging of DPPC, DPPE, DPPG, and DPPS Monolayers Caused by Dimethylsulfoxide Observed Using Brewster Angle Microscopy

Xiangke Chen, Zishuai Huang, Wei Hua, Hardy Castada, and Heather C. Allen*

Department of Chemistry, The Ohio State University, 100 West 18th Avenue, Columbus, Ohio 43210, United States

Received July 16, 2010. Revised Manuscript Received October 26, 2010

The interaction between dimethylsulfoxide (DMSO) and phospholipid monolayers with different polar headgroups was studied using “in situ” Brewster angle microscopy (BAM) coupled to a Langmuir trough. For a 1,2-dipalmitoyl-*sn*-glycero-3-phosphocholine (DPPC) monolayer, DMSO was shown to significantly impact the structure of the liquid expanded (LE) and gaseous phases. The domains reorganized to much larger domain structures. Domains in the liquid condensed (LC) phase were formed on the DMSO-containing subphase at the mean molecular area where only gaseous and LE phases were previously observed on the pure water subphase. These results clearly demonstrate the condensing and caging effect of DMSO molecules on the DPPC monolayer. Similar effects were found on dipalmitoyl phosphatidyl ethanolamine, glycerol, and serine phospholipids, indicating that the condensing and caging effect is not dependent upon the phospholipid headgroup structure. The DMSO-induced condensing and caging effect is the molecular mechanism that may account for the enhanced permeability of membranes upon exposure to DMSO.

Introduction

Biological membranes are not only a remarkable barrier to keep the cell intact, but they also allow exchange of necessary substances.^{1–3} Molecules that can selectively increase (or decrease) the permeability of membranes are of particular interest for many practical applications such as transdermal drug delivery.^{4,5} The well-organized membrane consists of lipid bilayers with interconnected gel and liquid-phase domains that result in a relatively low membrane permeability.⁴ An approach to enhancing membrane permeability is to perturb and temporarily disrupt the lipid domain structure with certain chemicals called penetration enhancers.⁶ To be a successful penetration enhancer in a clinic trial, the agent should be able to promote skin permeability, but also be nontoxic to humans. First introduced 40 years ago, dimethylsulfoxide (DMSO) is one of the oldest as well as the most widely used penetration enhancers.^{7,8}

The observed membrane permeability enhancement induced by DMSO seems to be nonspecific and applies to all membranes that consist of similar amphiphilic molecules, i.e., ceramides in skin and phospholipids in cells.⁵ Yet, how DMSO modifies lipid membrane structure and function, namely, the molecular-level interaction mechanism of DMSO on lipid membranes, is still under investigation.^{9,10} The research presented here sheds light on the underlying mechanism of DMSO-induced membrane permeability.

Although lipid molecules show considerable structural diversity, such as sterols, fatty acids, phospholipids, and glycolipids, the most important to the bilayer structure backbone are the phospholipids.¹ The amphiphilic structure of phospholipids gives rise to their unique ability to form elegant bilayers with the long alkyl chain tailgroups congregated together as a hydrophobic center and the charged headgroups facing out to the hydrophilic environment. Phospholipid bilayers can be formed from single constituents, such as dipalmitoylphosphatidylcholine (DPPC), dipalmitoylphosphatidylethanolamine (DPPE), dipalmitoylphosphatidylglycerol (DPPG), or dipalmitoylphosphatidylserine (DPPS), or multiple components of these. Despite the fact that all phospholipids contain a negatively charged phosphate in the headgroup, properties of phospholipids vary significantly due to polar groups attached to the phosphate. For example, the headgroups of DPPC and DPPE are zwitterionic, while the headgroups of DPPG and DPPS are net negatively charged as shown in Scheme 1. This difference in phospholipid headgroup results in different intermolecular interactions, leading to different packing ability.^{11,12} Due to the complexity of the membrane structure, simpler models such as lipid vesicles, lipid bilayers, and Langmuir monolayers are often studied.¹³ Among which, Langmuir monolayers formed at the air/water interface provide the most control, for example, a continuously well-defined molecular density, surface pressure, and phase.^{14,15}

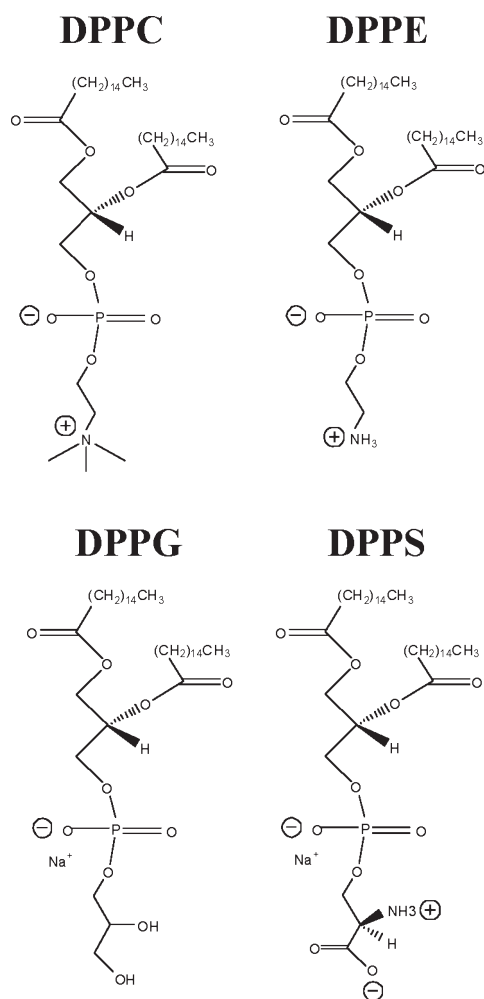
The interaction of DMSO with phospholipid membranes has been previously studied by various experimental and theoretical approaches, such as differential scanning calorimetry (DSC),^{16–19}

*allen@chemistry.ohio-state.edu.

(1) Singer, S. J.; Nicolson, G. L. *Science* **1972**, *175*, 720.
(2) Zubay, G. *Biochemistry*, 2nd ed.; Macmillan: New York, 1988; p 154.
(3) Edidin, M. *Nat. Rev. Mol. Cell Biol.* **2003**, *4*, 414.
(4) Barry, B. W. *Nat. Biotechnol.* **2004**, *22*, 165.
(5) Notman, R.; Noro, M.; O'Malley, B.; Anwar, J. J. *Am. Chem. Soc.* **2006**, *128*, 13982.
(6) Williams, A. C.; Barry, B. W. *Adv. Drug Delivery Rev.* **2004**, *56*, 603.
(7) Jacob, S. W. *Curr. Ther. Res., Clin. Exp.* **1964**, *6*, 134.
(8) Kligman, A. M. *J. Am. Med. Assoc.* **1965**, *193*, 796.
(9) Gurtovenko, A. A.; Anwar, J. J. *Phys. Chem. B* **2007**, *111*, 10453.
(10) Chen, X. K.; Allen, H. C. *J. Phys. Chem. A* **2009**, *113*, 12655.

(11) Lindblom, G.; Rilfors, L.; Hauksson, J. B.; Brentel, I.; Sjolund, M.; Bergenstahl, B. *Biochemistry* **1991**, *30*, 10938.
(12) Minones, J.; Patino, J. M. R.; Conde, O.; Carrera, C.; Seoane, R. *Colloid Surf., A: Physicochem. Eng. Asp.* **2002**, *203*, 273.
(13) Berkowitz, M. L.; Bostick, D. L.; Pandit, S. *Chem. Rev.* **2006**, *106*, 1527.
(14) Phillips, M. C.; Chapman, D. *Biochim. Biophys. Acta* **1968**, *163*, 301.
(15) Paltauf, F.; Hauser, H.; Phillips, M. C. *Biochim. Biophys. Acta* **1971**, *249*, 539.
(16) Yu, Z. W.; Quinn, P. J. *Biophys. J.* **1995**, *69*, 1456.

Scheme 1. Molecular Structures of the Studied Phospholipids



X-ray diffraction (XRD),^{16,17,20,21} small-angle neutron diffraction,^{22,23} nuclear magnetic resonance (NMR),²⁴ infrared (IR) spectroscopy,¹⁸ and molecular dynamics (MD) simulations.^{5,25–28} The influence of DMSO on membranes was shown to be concentration-dependent.²⁰ In a water/DMSO mixed solvent, the main phase transition temperature of DPPC vesicles increases with DMSO concentration, revealing a stabilization effect by DMSO on the vesicle gel phase.¹⁶ X-ray and neutron diffraction studies revealed that the repeat distance between the bilayers in multilamellar DPPC vesicles decreased with DMSO concentration. This decrease in intermembrane distance inside the vesicles was mainly attributed to the removal of free water molecules in

the intermembrane spaces.^{20,23} In addition, Sum et al. showed through MD simulations that DMSO penetrates readily into the polar headgroup region of a bilayer, but only a few DMSO molecules actually cross the bilayer.²⁸ Recently, Anwar and co-workers reported that DMSO induces water pore formation within a DPPC bilayer by MD simulation, which presented an interesting mechanism for transdermal permeability enhancement.^{5,9} In our recent work, the interaction between a DPPC monolayer and DMSO was investigated using vibrational sum frequency generation (VSFG). Results suggested that DPPC monolayers adopt a more condensed packing state at high DMSO concentration, giving room for channel formation inside a membrane.¹⁰

Brewster angle microscopy (BAM) is a surface-sensitive optical technique suitable for “in situ” studies of phospholipid monolayers.^{29,30} Through coupling with a Langmuir trough, this method is capable of visualizing characteristic domain structures of the monolayer in various phases. The aim of this work is to employ BAM to study the impact of DMSO on the monolayer morphology of various phospholipids, including DPPC, DPPE, DPPG, and DPPS, through which a global view of the interaction between DMSO and cellular membrane lipids is obtained.

Experimental Section

Materials. 1,2-Dipalmitoyl-*sn*-glycero-3-phosphocholine (DPPC), 1,2-dipalmitoyl-*sn*-glycero-3-phosphoethanolamine (DPPE), 1,2-dipalmitoyl-*sn*-glycero-3-phosphoglycerol sodium salt (DPPG), and 1,2-dipalmitoyl-*sn*-glycero-3-phospho-L-serine sodium salt (DPPS) were purchased from Avanti Polar Lipids (Alabaster, AL). Spectrophotometric-grade chloroform and methanol were purchased from Fisher Scientific and used as a mixed solvent for spreading of the phospholipids. Molecular structures are shown in Scheme 1. The concentration of phospholipid stock solutions was ~1 mM. DMSO (>99% purity) was purchased from Fisher. Deionized water (not purged of CO₂) with a resistivity of 18.2 MΩ·cm and a measured pH of 5.5 was from a Barnstead Nanopure system.

Langmuir Trough. The surface pressure–area isotherm was obtained with a KSV minitrough (KSV, Finland). The rectangular trough (176.5 mm × 85 mm) is made of Teflon, and two barriers are employed to provide symmetric film compression. The barriers, which are made of Delrin, prevent leakage of the monolayer. The surface pressure and mean molecular area were continuously monitored during film compression by the Wilhelmy plate method. The trough was filled with Nanopure water as the subphase. The surface pressure–area isotherm was always measured on a fresh water or 0.1x (mole fraction) DMSO subphases. The compression rate of the barrier to obtain the isotherms was 5 mm/min. Before recording an isotherm, the surface pressure was zeroed for each subphase. The sample temperature was maintained at 22 ± 1 °C for isotherm and in situ BAM measurements.

Brewster Angle Microscopy. The BAM experiments were carried out on a self-assembled symmetric goniometer system. The laser light source is from Research Electro-Optics, Inc., and emits 17 W at 633 nm, which is incident at the Brewster angle of the subphase, i.e., 53.1° for water. The incident beam is attenuated by a neutral density filter and passes through a half-wave plate before reaching the liquid surface. An infinity-corrected 20× Nikon lens together with a tube lens are used to form the image. The BAM image is collected on an Andor charge-coupled device (CCD; Andor DV412) of 512 × 512 pixels. The scale of BAM image is 350 μm × 350 μm.

(17) Tristram-Nagle, S.; Moore, T.; Petrache, H. I.; Nagle, J. F. *Biochim. Biophys. Acta* **1998**, *1369*, 19.

(18) Long, C. J.; Hmel, P. J.; Kennedy, A.; Quiles, J. G.; Seelbaugh, J.; Reid, T. J. *J. Liposome Res.* **2003**, *13*, 249.

(19) Kiselev, M. A.; Gutberlet, T.; Lesieur, P.; Hauss, T.; Ollivon, M.; Neubert, R. H. H. *Chem. Phys. Lipids* **2005**, *133*, 181.

(20) Kiselev, M. A.; Lesieur, P.; Kiselev, A. M.; Grabielle-Madmond, C.; Ollivon, M. *J. Alloy. Compd.* **1999**, *286*, 195.

(21) Krasteva, N.; Vollhardt, D.; Brezesinski, G.; Mohwald, H. *Langmuir* **2001**, *17*, 1209.

(22) Gorshkova, J. E.; Gordeliy, V. I. *Crystallogr. Rep.* **2007**, *52*, 535.

(23) Kiselev, M. A. *Crystallogr. Rep.* **2007**, *52*, 529.

(24) Kennedy, A.; Long, C. J.; Hmel, P. J.; Hicks, R.; Reid, T. J. *Spectrosc. Int. J.* **2004**, *18*, 265.

(25) Paci, E.; Marchi, M. *Mol. Simul.* **1994**, *14*, 1.

(26) Smondyrev, A. M.; Berkowitz, M. L. *Biophys. J.* **1999**, *76*, 2472.

(27) Sum, A. K.; de Pablo, J. J. *Biophys. J.* **2003**, *85*, 3636.

(28) Leekumjorn, S.; Sum, A. K. *Biochim. Biophys. Acta* **2006**, *1758*, 1751.

(29) Henon, S.; Meunier, J. *Rev. Sci. Instrum.* **1991**, *62*, 936.

(30) Honig, D.; Mobius, D. *J. Phys. Chem.* **1991**, *95*, 4590.

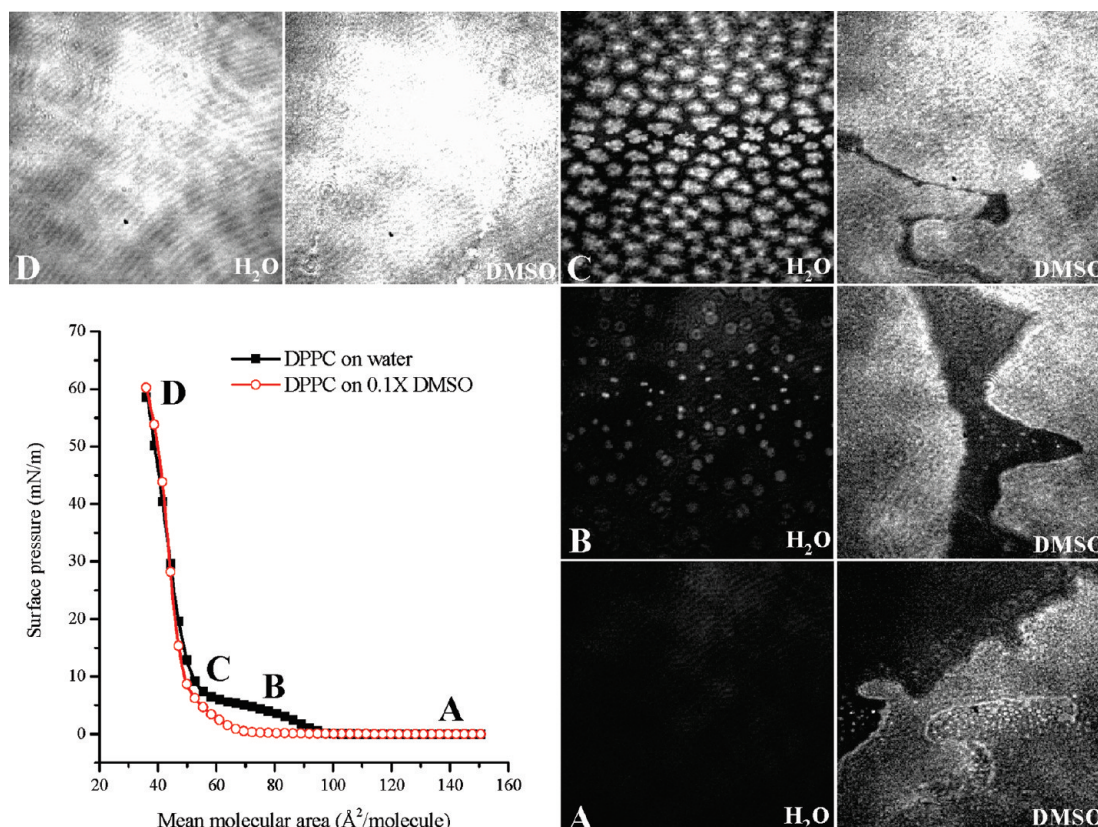


Figure 1. Surface pressure–area isotherms of DPPC monolayer on water and 0.1x (mole fraction) DMSO subphases at 22 °C. The BAM images of corresponding points on isotherms are shown in sets of two: A, B, C, and D. For each set of BAM images, the left image is on the water subphase, while the right image is on the 0.1x DMSO subphase. The image scale is $350\ \mu\text{m} \times 350\ \mu\text{m}$.

Results and Discussion

DPPC Monolayer. The BAM images of phospholipids on water and 0.1x DMSO subphases are shown together to visualize the impact of DMSO on the morphology of the phospholipid domains. Upon addition of DMSO, the refractive index of the interface increases to 1.37 on 0.1x DMSO from 1.33 on water,³¹ which corresponds to a Brewster angle change to 53.8° from 53.1° . The contrast in BAM images is based on the difference of refractive index of monolayer domains and the subphase. For the same phospholipid monolayer with full surface coverage, the contrast observed on a water subphase is more than 2 times that of the contrast observed on a 0.1x DMSO subphase, which suggests that the refractive index of the monolayer domains is greater than that of water. Moreover, no contrast (homogeneously dark image) is observed for phospholipids spread on a 0.2x DMSO subphase (image not shown). This indicates that the refractive index of monolayer domains is equal to that of the subphase, which is 1.40. Therefore, to compare the images taken on water and 0.1x DMSO subphases, the contrast (dark to bright) scale is set to 100 counts on water and 50 counts on 0.1x DMSO subphases. In addition, because the surface may not be homogeneous and the film domains move laterally on the aqueous surface, the images shown are not able to be exactly reproduced. Only typical images which represent the surface characteristics are therefore shown in the following results.

The surface pressure–area isotherms of a DPPC monolayer on water and 0.1x DMSO subphases are shown in Figure 1. DPPC exhibits interesting phase transition properties on water at room temperature. Several distinct phases, the gas–liquid expanded

coexistence region (G-LE, $> 100\ \text{\AA}^2$), the liquid expanded (LE, $75\text{--}100\ \text{\AA}^2$) phase, the liquid expanded–liquid condensed coexistence region (LE-LC, $\sim 55\text{--}75\ \text{\AA}^2$), and the liquid condensed (LC, $< 55\ \text{\AA}^2$) phase, and the collapse phase (not shown, $< 40\ \text{\AA}^2$) are observed (black square trace).³² As the DPPC monolayer is compressed to the LE phase, the surface pressure (difference between the surface tension of the subphase and the monolayer covered surface) begins to rise. The LE-LC phase transition plateau occurs at about 5 to 6 mN/m, which is considered to be a first-order phase transition.³³ However, the transition plateau is not perfectly horizontal, which seems to be inconsistent with a first-order transition. Previous studies on DPPC monolayers show that this nonzero transition slope can be caused by two factors:^{33,34} (1) there are impurities in the monolayer, or (2) the compression speed is not slow enough for the phase transition to occur in equilibrium. The compression rate used in the present study was 5 mm/min for each barrier, which corresponds to a rate of $8.5\ (\text{\AA}^2/\text{molecule})/\text{min}$ or higher. This is higher than the sufficiently slow compression rate of $0.1\ (\text{\AA}^2/\text{molecule})/\text{min}$ reported previously. After entering the LC phase, the surface pressure increases abruptly with compression, indicating a more rigid packing state of DPPC molecules.

The corresponding BAM images of DPPC in each phase on water and 0.1x DMSO subphases are also shown in Figure 1. Each set of images (A, B, C, and D; left image is on water subphase, while the right image is on 0.1x DMSO subphase) represents the typical morphology of a DPPC monolayer at the indicated mean molecular area (MMA). At MMA of $140\ \text{\AA}^2/\text{molecule}$

(32) Ma, G.; Allen, H. C. *Langmuir* **2006**, *22*, 5341.

(33) Hifeda, Y. F.; Rayfield, G. W. *Langmuir* **1992**, *8*, 197.

(34) Pallas, N. R.; Pethica, B. A. *Langmuir* **1985**, *1*, 509.

(31) Markarian, S. A.; Terzyan, A. M. *J. Chem. Eng. Data* **2007**, *52*, 1704.

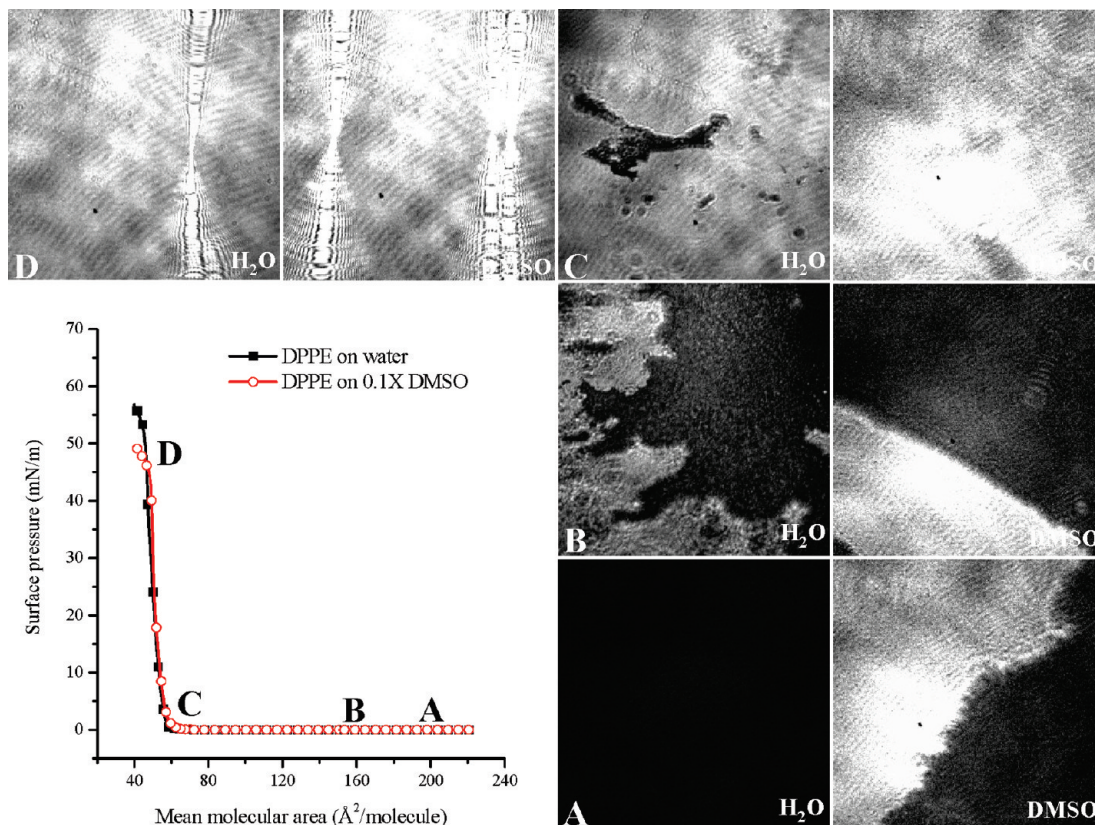


Figure 2. Surface pressure–area isotherms of DPPE monolayer on water and 0.1x DMSO subphases at 22 °C. The BAM images of corresponding points on isotherms are shown in sets of two: A, B, C, and D. For each set of BAM images, the left image is on water subphase while the right image is on the 0.1x DMSO subphase. The image scale is $350 \mu\text{m} \times 350 \mu\text{m}$.

(Figure 1A), the image is completely dark, which indicates a homogeneous G-LE coexistence region. A similarly dark image is observed for the LE phase at the surface pressure of 4 mN/m (image not shown), revealing that the LE phase is also homogeneous. This observation is similar to the BAM images reported by Minones et al.¹² However, they observed an average reflectivity increase from the G-LE region to the LE phase, despite the same homogeneous feature of these two regions. The brightness of the images is monitored to be the same for these two regions in the present study. Previous vibrational sum frequency generation (VSFG) studies completed in our group³² show that VSFG spectra intensities can be detected when entering the LE phase (surface pressure > 0.1 mN/m). Because VSFG is sensitive to ordering of molecules, it can therefore be concluded that DPPC molecules are beginning to order at the onset of the LE phase, although the G-LE coexistence phase is dominated by disorder. The homogeneous nature of the LE phase image suggests that the LE phase is still monomer-rich although molecules are becoming more ordered. Therefore, a significant change in surface reflectivity is not expected.

At the surface pressure of 4.5 mN/m ($\text{MMA} = 75 \text{ \AA}^2/\text{molecule}$), the kink point between LE phase and LE-LC transition region is reached. Small, circular domains of DPPC appear instantaneously (Figure 1B) as the phase transition commences. These LC phase domains are bright in contrast (counts > 50) with domain sizes of around $10 \mu\text{m}$ in diameter (nonuniform focus somewhat distorts the size of the domain in the outer edges of the image). The large increase in contrast from the dark LE phase (counts < 15) to the bright LC phase reveals the different packing density in these phases. LC domains are cluster-rich and less compressible, hence resulting in a greater refractive index than the

LE phase. In the phase transition region, the circular LC domains grow in size to $30\text{--}40 \mu\text{m}$ and form irregular lobe shapes (Figure 1C). This kind of shape is typically observed in fluorescence microscopy and is considered to be caused by the chirality of the DPPC molecules. Once the LE-LC transition region is exceeded, the domains merge together with an abrupt increase in surface pressure, and the lobe shape slowly disappears. At the end of compression (Figure 1D), the DPPC monolayer becomes homogeneous again, but with much greater brightness (counts > 100).

When DPPC is spread on a 0.1x DMSO subphase, the spreading of DPPC at the surface is slower than on water. The surface pressure–area isotherm shows significant differences from that of the water subphase images as seen in Figure 1. The LE-LC transition plateau nearly disappears and the DPPC monolayer undergoes a direct G-LC phase transition as being compressed in accordance with previous studies.^{21,35} However, the DPPC monolayer exhibits similar LC phase morphology on both water and 0.1x DMSO subphases as observed in Figure 1D, which indicates the exclusion of DMSO molecules out of the condensed monolayer. This observation is also in accordance with previous VSFG¹⁰ and NMR studies.²⁴

The BAM images shown in Figure 1A, B, C, and D visualize the change in the isotherms. Excessively large domain structures and phase boundaries are formed on 0.1x DMSO subphase at $\text{MMA} = 140 \text{ \AA}^2/\text{molecule}$ (Figure 1A) as compared to the all-dark gaseous state on water. The brightness of the domains reveals that

(35) Haberlandt, R.; Michel, D.; Poppl, A.; Stannarius, R. *Lecture Notes in Physics: Molecules in Interaction with Surfaces and Interfaces*; Springer: New York, 2004; Vol. 634, p 435.

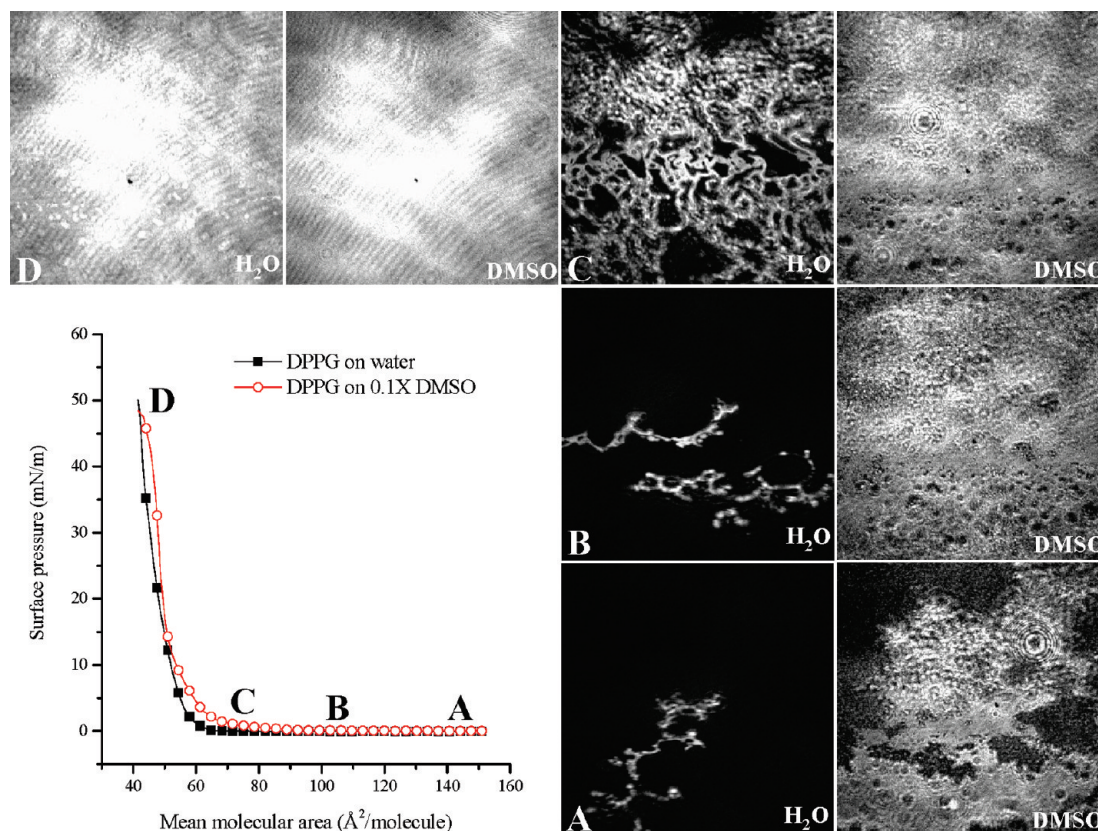


Figure 3. Surface pressure–area isotherms of DPPG monolayer on water and 0.1x DMSO subphases at 22 °C. The BAM images of corresponding points on isotherms are shown in sets of two: A, B, C, and D. For each set of BAM images, the left image is on water subphase while the right image is on the 0.1x DMSO subphase. The image scale is $350 \mu\text{m} \times 350 \mu\text{m}$.

the domains are predominately in the LC phase. In between the large coalesced domain structures, small circular DPPC domains are also observable. The existence of LC domains indicates the presence of the G-LC coexistence state at this large MMA. Our recent VSFG study of a DPPC monolayer on DMSO containing subphases also pointed to the existence of ordered domains at the MMA of $120 \text{ \AA}^2/\text{molecule}$.¹⁰ The formation of LC domains at such large MMA is attributed to the condensing effect of DMSO on DPPC monolayer. Another way to view the action of DMSO is that these molecules act to cage or corral the DPPC molecules into larger domain LC phase DPPC structures that then leave larger regions free of the LC phase DPPC.

Due to the amphiphilic nature of the DMSO molecule, DMSO molecules show a preference for the aqueous surface. The DMSO molecules occupy large surface regions and exert pressure on the DPPC molecules forcing them to congregate. As the concentration of DMSO exceeds 0.1x, the surface pressure of the subphase alone is 10 mN/m ,³¹ which is greater than the DPPC LE-LC transition surface pressure for DPPC on water. Therefore, the DPPC monolayer is condensed by surface DMSO molecules and the LC domains are formed on the 0.1x DMSO subphase no matter what the MMA is. These LC domains coexist with the gaseous-phase DPPC at large MMA.

As the DPPC monolayer is compressed on the 0.1x DMSO subphase, the LC domains coalesce and gradually merge together. No instantaneous phase transition such as the LE-LC transition on the water subphase is observed (Figure 1B,C), revealing the continuous evolution from the G-LC coexistence region to the LC phase. Similar homogeneous condensed-phase DPPC monolayers are observed on both water and 0.1x DMSO subphases (Figure 1D). In addition, some collapse structures such as stripes

and dots are also visible when the surface pressure rises above 50 mN/m .

DPPE Monolayer. Figure 2 shows the surface pressure–area isotherms of a DPPE monolayer on water and 0.1x DMSO subphases. The difference between DPPE and DPPC molecules is that the ammonium group in DPPE is fully methylated to the *N,N,N*-methyl amine group. Unlike the methyl groups on the DPPC headgroup, the hydrogens on the DPPE ammonium group can form hydrogen bonds with neighboring DPPE headgroups. This is thought to account for the more stable DPPE monolayer than the DPPC monolayer, which is evidenced by the higher main transition (gel phase to liquid crystalline phase) temperature of DPPE bilayers ($63 \text{ }^\circ\text{C}$) than DPPC bilayers ($41 \text{ }^\circ\text{C}$).³⁶ Therefore, the DPPE molecules more easily interact with each other to form domains. In the surface pressure–area isotherm on water, the DPPE monolayer goes directly through the G-LC coexistence phase to the LC phase, and no LE phase is observed. The isotherm on the 0.1x DMSO subphase shows the same character, which suggests that the DMSO molecules have little effect on the condensed DPPE monolayer.

The BAM images of DPPE monolayer at different MMAs are shown in Figure 2A,B,C,D. On the water subphase, a pure gaseous phase (dark contrast) is observed when the MMA is greater than $170 \text{ \AA}^2/\text{molecule}$ as shown in Figure 2A. At around $170 \text{ \AA}^2/\text{molecule}$, irregular LC domain structures are formed (Figure 2B) although the surface pressure is still nearly zero. This MMA should be attributed to the G-LC coexistence region. However, on the 0.1x DMSO subphase the large LC domain structures of the DPPE monolayer are clearly observable

(36) Mason, J. T.; Oleary, T. J. *Biophys. J.* **1990**, *58*, 277.

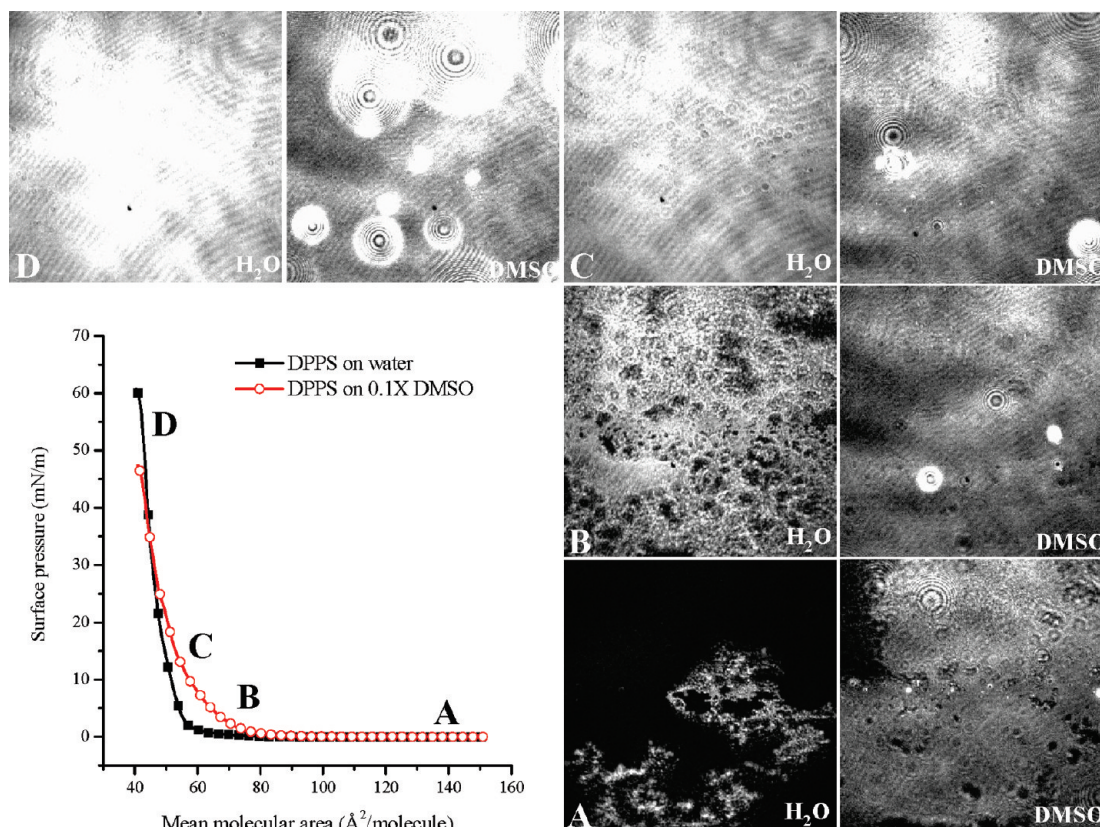


Figure 4. Surface pressure–area isotherms of DPPS monolayer on water and 0.1x DMSO subphases at 22 °C. The BAM images of corresponding points on isotherms are shown in sets of two: A, B, C, and D. For each set of BAM images, the left image is on water subphase while the right image is on the 0.1x DMSO subphase. The image scale is $350 \mu\text{m} \times 350 \mu\text{m}$.

(Figure 2A) at the MMA where only pure gaseous phase is seen on water. This observation suggests that DMSO molecules on the aqueous surface cause the condensation of DPPE molecules to form condensed-phase domain structures, which is similar to the effect on the DPPC monolayer.

When the DPPE monolayer on 0.1x DMSO is compressed to the LC phase, a homogeneously condensed monolayer is gradually formed. Finally, the bright collapse state is observed in Figure 2C, and the three-dimensional stripe structures are seen in Figure 2D.

DPPG Monolayer. The surface pressure–area isotherms of net negatively charged DPPG monolayers on water and 0.1x DMSO subphases are shown in Figure 3. The shape of the isotherms is similar to that of the DPPE monolayers. As the DPPG monolayer is compressed, only a G-LC coexistence region and the LC phase are observed. The MMA of the onset of the DPPG LC phase is between 50 and 60 $\text{\AA}^2/\text{molecule}$, which is about the same as the DPPC and DPPE monolayers.¹²

As seen from the BAM images of the DPPG monolayer on a water subphase, irregular branch-shaped LC domains exist on the water surface (Figure 3A,B). These LC domains interconnect with each other as the monolayer is compressed (Figure 3C) and a homogeneous LC phase monolayer is formed when the surface pressure is greater than 40 mN/m (Figure 3D). On the 0.1x DMSO subphase, the morphology of the LC domains in the G-LC coexistence region is markedly different despite the similar isotherms. Large domain structures of interconnected islands hundreds of micrometers in diameter are observed in Figure 3A. These LC phase islands appear porous, as the dark gaseous phase coexists with the bright domain structures. The larger size of the LC domains observed on the 0.1x DMSO subphase as compared

to water suggests that the DPPG domains are forced to grow and merge together on the 0.1x DMSO subphase. This is in accordance with the condensing and caging effect of DMSO on the zwitterionic DPPC and DPPE monolayers, although DPPG is a negatively charged lipid.

DPPS Monolayer. DPPS is another important negatively charged phospholipid. It has three charged centers on the head-group at physiological pH: the negatively charged phosphate and carboxylic groups, and the positively charged ammonium group.³⁷ According to previous study, the isoelectric point of DPPS is at a pH of 1.5.³⁸ At this pH, the carboxylic group of DPPS is completely protonated so that the DPPS molecule becomes zwitterionic. The main transition temperature of a DPPS bilayer is found to be 51 °C, which is higher than DPPG (40 °C).³⁹ The intermolecular attractions between the DPPS carboxylic group and the ammonium group are thought to be the cause for the assembly of DPPS molecules at zero surface pressure,¹² resulting in the G-LC coexistence region in the isotherms.

The surface pressure–area isotherms of a DPPS monolayer on water and 0.1x DMSO subphases are similar to the DPPG monolayer as shown in Figure 4. In both DPPS isotherms on different subphases, only the G-LC coexistence and LC phases are observed. Changing from water to 0.1x DMSO in the subphase shows insignificant impact on the isotherms.

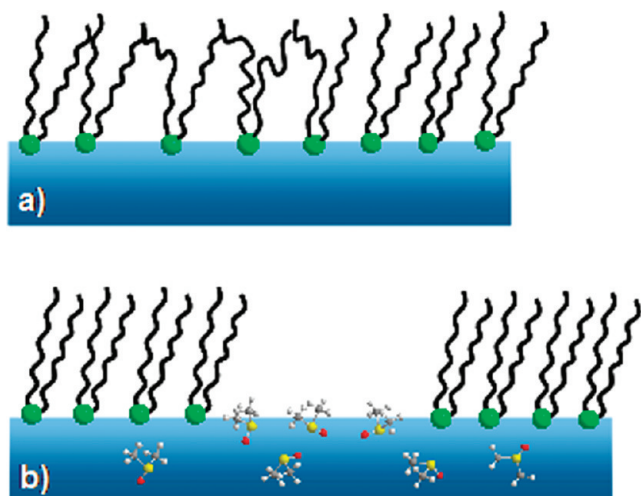
However, the changes are observed for the DPPS monolayer on different subphases as revealed in the corresponding BAM images in Figure 4. Although the morphology of the LC domains

(37) Seimiya, T.; Ohki, S. *Nat. New Biol.* **1972**, 239, 26.

(38) Hauser, H.; Darke, A.; Phillips, M. C. *Eur. J. Biochem.* **1976**, 62, 335.

(39) Jing, W. G.; Prenner, E. J.; Vogel, H. J.; Waring, A. J.; Lehrer, R. I.; Lohner, K. *J. Pept. Sci.* **2005**, 11, 735.

Scheme 2. Illustration of the Proposed Impact of DMSO Molecules on the DPPC Monolayer Structure in the Situation of an Unconfined Monolayer Area^a



^a (a) Coexistence of condensed and expanded lipid domains in the absence of DMSO molecules. (b) In the presence of DMSO molecules, the competition of DMSO molecules at the surface causes condensation of the DPPC monolayer, as well as an increase in the overall monolayer area.

is somewhat similar on both subphases, the area covered by the domains is greater on the 0.1x DMSO subphase. In addition, some very bright dots are clearly seen in the interior of the DPPS domains on the 0.1x DMSO subphase, and attributed to collapsed DPPS three-dimensional structures. Therefore, it can also be concluded that the DMSO molecules cause condensation and caging of DPPS.

The four phospholipids studied here account for the major components of cell membranes. The observed condensing and caging effect by DMSO on these phospholipids has implications for understanding the molecular-level details of the enhanced permeability of biological membranes. Previous MD simulations of a DPPC bilayer in a DMSO-containing subphase suggests that transient water pores could be formed inside the DPPC bilayer, which then enhances the permeability of the membrane.⁵ This permeability effect could possibly be a result of the condensing and caging effect of DMSO molecules on the phospholipid monolayers. When the DMSO molecules interact with the phospholipid

membranes, DMSO molecules squeeze aside the phospholipids due to the DMSO surface activity. When the surface area of the monolayer is defined (i.e., in a Langmuir trough as in this study), surface-residing DMSO molecules cause the phospholipids to condense. For unconfined monolayers (similar to the bilayers in vesicles or tissues), the presence of surface DMSO molecules can induce tightly packed domain structures, in accordance with the decreased compressibility as shown by MD simulation,⁵ but also cause the monolayer to expand. Namely, although the individual lipid domains are more well-defined, the overall monolayer integrity is disrupted as shown in Scheme 2. In addition, the miscibility of DMSO with water⁴⁰ and its powerful solvation of many substances make the DMSO-occupied surface area a transportation corridor across the membrane. Moreover, as shown in this research, the DMSO–phospholipid interaction is strong, not lipid-structure specific, and affects phospholipid headgroups with different chemical properties.

Conclusions

In situ Brewster angle microscopy (BAM) together with surface pressure–area isotherm measurement are used to investigate the condensing and caging effect of DMSO molecules on different phospholipid monolayers. It is found that on the 0.1x DMSO subphase, phospholipids form large condensed domain structures readily, and the two-dimensional structures formed usually have large areas, greater than hundreds of micrometers in diameter. When the phospholipid monolayers are compressed to high surface pressures of over 40 mN/m, DMSO molecules are squeezed out of the monolayers. The observed condensing effect of DMSO molecules on phospholipids physically changes the morphology of the film, creating DMSO-rich and lipid-poor regions. Moreover, DMSO affects phospholipids with different chemical substituents and the observed caging effect can therefore be generalized for many lipid types. The physical interaction between DMSO molecules and phospholipids possibly accounts for the enhanced permeability of biological membranes induced by DMSO molecules.

Acknowledgment. The authors thank the National Science Foundation (NSF-CHE) for supporting this work. We also thank Jim Rathman for his assistance in the BAM experimental setup.

(40) Shashkov, S. N.; Kiselev, M. A.; Tioutiunnikov, S. N.; Kiselev, A. M.; Lesieur, P. *Physica B* **1999**, *271*, 184.